ANL/ER/CP--86429
CONF-950450--8

Integration of Geophysics within the Argonne Expedited Site Characterization Program at a Site in the Southern High Plains

by

Bruce Hastings, George Hildebrandt, Tim Meyer,

Wayne Saunders, Jacqueline C. Burton

Argonne National Laboratory

Argonne Expedited Site Characterization Program

DISCLAIMER

Short Title: Argonne ESC in Southern High Plains

Integration of Geophysics within the Argonne Expedited Site Characterization Program at a Site in the Southern High Plains

by

Bruce Hastings, George Hildebrandt, Tim Meyer,

Wayne Saunders, Jacqueline C. Burton

Argonne National Laboratory

Argonne Expedited Site Characterization Program

ABSTRACT

An Argonne National Laboratory Expedited Site Characterization (ESC) program was carried out at a site in the central United States. The Argonne ESC process emphasizes an interdisciplinary approach in which all available information is integrated to produce as complete a picture as possible of the geologic and hydrologic controls on contaminant distribution and transport. As part of this process, all pertinent data that have been collected from previous investigations are thoroughly analyzed before a decision is made to collect additional information.

A seismic reflection program recently concluded at the site had produced inconclusive results. Before we decided whether another acquisition program was warranted, we examined the existing data set to evaluate the quality of the raw data, the appropriateness of the processing sequence, and the integrity of the interpretation. We decided that the field data were of sufficient quality to warrant reprocessing and reinterpretation.

The main thrust of the reprocessing effort was to enhance the continuity of a shallow, low-frequency reflection identified as a perching horizon within the Ogallala

formation. The reinterpreted seismic data were used to locate the boundaries of the perched aquifer, which helped to guide the Argonne ESC drilling and sampling program. In addition, digitized geophysical well log data from previous drilling programs were reinterpreted and integrated into the geologic and hydrogeologic model.

INTRODUCTION

The site is located in the southern High Plains, an 80,000-km^2 remnant of the alluvial plain formed east of the Rocky Mountains during Miocene and possibly Pliocene time. The detritus making up this alluvial plain ranges from locally coarse fluvial gravel in the lower part to fluvial and eolian sand, silt, and clay in the upper part. This sequence, which constitutes the Ogallala Formation, is underlain by Permo-Triassic bedrock and overlain by silts and clays.

An unconfined aquifer in the sands of the lower Ogallala is a principal source of water in the southern High Plains area. In the vicinity of the site, this main aquifer lies about 350-425 ft below the surface. The saturated thickness of the Ogallala aquifer northeast of the site exceeds 300 ft, placing it among the thickest sections in the region.

At the site, groundwater occurs at two levels, directly above the bedrock and in a shallower perched zone. The lower aquifer is a major source of drinking water in the surrounding area. The perched water zone is significant because of the organic and inorganic contaminants in it and their potential to migrate downward into the Ogallala aquifer. Although both water zones occur in the Ogallala Formation, the convention at the site is to refer to the shallow perched zone as the perched aquifer and the deeper zone as the Ogallala aquifer. That terminology is used in this paper.

Past reports indicated that a thick, continuous caliche layer lay beneath the site. This layer was believed to inhibit vertical flow in the vadose zone. The aquitard beneath the perched aquifer is reported to be a persistent zone of low-permeability, fine-grained

material. Drillers' logs generally describe the aquitard as consisting primarily of clays, clayey silts, and sands.

On a regional level, recharge into the Ogallala aquifer takes place both through diffusive infiltration directly into Ogallala outcrops and through Quaternary deposits that overlie the Ogallala. Focused recharge may also occur locally in playa lakes or riverbeds. Four playas are within the site boundary, and six more are within one mile of the plant. These topographic depressions average about one mile across, with ephemeral lakes in their centers. One of the playas at the site contains water all year.

Review of seismic data

A number of surface geophysical studies have been undertaken in and around the site, and geophysical logs have been run in many boreholes. Over 17 miles of surface seismic lines have been acquired, processed, and interpreted as part of a site-wide hydrogeologic study.

A preliminary review of the seismic reflection data revealed that certain steps in the processing and interpretation of the data could be improved. The data were originally acquired with instruments and filter settings that reduced the frequency bandwidth and altered the phase of the data. The data were subsequently processed with computer algorithms and processing parameters that may have artificially aligned essentially random noise, thus reducing the overall signal-to-noise ratio. Finally, interpreted stratigraphic horizons were not tied at line intersections, resulting in inconsistent maps.

Acquisition

The original seismic reflection program was designed to image several important lithologic and hydrogeologic targets, including the overlying silts and clays, the Ogallala Formation (with emphasis on the aquitard within the Ogallala, the suspected caliche layer, the top of the perched aquifer, and the top of the Ogallala aquifer), and bedrock. The parameters selected for the program are presented in Table 1.

The acquisition parameters were intended to provide a high-frequency reflection signal and to reduce the amount of low-frequency surface noise. A low-cut field filter was selected to attenuate frequencies below 50 Hz, and geophones were selected with a resonant frequency of 100 Hz. Single geophones were spaced 10 ft apart.

Processing

The original processing of the data was subcontracted to a seismic processing firm. The processing sequence used by this firm is shown in Table 2. No attempt was made in the Argonne ESC to recreate the original processing sequence. Rather, Argonne's efforts were focused on completely reanalyzing the raw field data.

Three aspects of the original seismic processing flow deserve special attention. The first is the application of a spectral balancing algorithm fairly early in the processing sequence (step 7 in Table 2). The spectral balancing process originally applied to the data apparently was designed to boost the high frequencies to the point where the frequency spectrum became essentially flat at 30-240 Hz. However, the Argonne ESC reprocessing showed that the bandwidth of the actual signal was approximately 20-90 Hz, with a peak around 30 Hz, so the primary effect of balancing the spectrum to 240 Hz was to amplify high-frequency noise in the range of 90-240 Hz.

Figure 1 shows a field record from the original seismic data set. The only processing applied to this record was trace editing and automatic gain recovery. The reflections can be seen on traces 35-70 between the first break at the top of the record and the surface noise at the bottom.

Figure 2 shows a spectral analysis of traces 35-70 from the field record displayed in Figure 1. Examination of the frequency content of the traces at 0-500 ms suggests that the legitimate signal energy might indeed extend to 200 Hz and beyond. However, examination of the frequency content of only the reflections (Figure 3) gives a much different impression. The bandwidth of the reflection signal appears to be much more restricted, being concentrated approximately between 20 Hz and 90 Hz, except for a noise spike at 120 Hz.

Figures 4a and b, respectively, show the same field record after the application of a spectral balancing process at 30-90 Hz and another at 30-240 Hz. The reflectors are much stronger and more continuous with the more conservative (30-90 Hz) spectral balancing (Figure 4a), demonstrating that the frequency band at 90-240 Hz contains a high proportion of noise.

A second feature of the original processing sequence was the repeated application of various statics correction routines. The ground surface at the site is relatively flat and, except around the playas, of relatively uniform near-surface velocity. Reprocessing during the Argonne ESC indicated that a reasonable seismic section could be produced without the application of any static corrections. In the original processing, however, the processing firm apparently applied three correlation-based automatic static corrections to the data (steps 14, 18, and 19 in Table 2), in addition to elevation ("datum") corrections (step 10) and static corrections (step 13) derived from analysis of the first-break arrival times. A casual examination of the linearity of the first breaks on representative field records (Figure 1) suggests that such statics correction efforts were unwarranted. The primary effect of this

repeated application of static correction programs may have been to artificially produce coherent alignment of otherwise incoherent high-frequency noise.

Finally, a random noise suppression filter (step 22 in Table 2) was applied after the data were stacked (summed). It is impossible to evaluate the effect of the random-noise suppression filter alone, but such enhancement filters must be used with care, because they cannot discriminate between the types of data being enhanced. If the signal-to-noise ratio is sufficiently poor at the outset, such filters may cause spurious lineups of essentially random noise.

Interpretation

Processed seismic sections were originally interpreted on the top and at the base of a shallow caliche layer, on the top and at the base of the aquitard, and on a Permo-Triassic ("red bed") bedrock surface. Cross-sections showing the elevations of these units were constructed along each seismic line, and contour maps were made of the depth to the caliche, the aquitard thickness, and the depth to bedrock. Interpretations were tied to subsurface data where seismic lines crossed the locations of boreholes for which lithologic logs were available.

Our examination of the seismic sections indicated that consistent seismic reflections correlated with the aquitard or with bedrock in only a few locations. The reflection identified as caliche was continuous in places but was absent or discontinuous elsewhere.

The original interpretation itself appears to suffer from other inconsistencies. The interpreted depth scales do not seem to correlate with the depths derived from the geophysical velocity profile (see Figure 5). In addition, the interpreted horizons on the seismic lines do not tie at several of the line intersections. An example of such a mis-tie is shown in Figure 6. Consequently, the contour maps exhibit inconsistencies that cannot be resolved without reinterpretation of the sections.

ARGONNE ESC REPROCESSING

Argonne reprocessed several lines of the original data set. Two of the reprocessed lines, B-1 and B-3, are shown in Figures 7a and b, respectively The data were reprocessed by using SEISTRIX-E from Interpex, Ltd., a personal computer, DOS-based seismic processing system.

The processing sequence used in the Argonne ESC is shown in Table 3. Extensive filter tests of selected data sets using the original sample interval (0.5 ms) indicated that no useful reflection energy existed above 80 Hz. To save disk space and speed processing, the data were subsequently resampled to 2 ms after a 125-Hz anti-alias filter was applied.

The use of analog recording filters and geophones with 100-Hz resonant frequencies in the data acquisition had apparently distorted the phase of the recorded signal. For example, a double-peaked reflection signature was uniformly observed at the top of the perched aquifer, where the geophysics would predict a single, large-amplitude, positive reflection. Spiking deconvolution seemed to provide the best improvement in overall signal quality. Surface-consistent deconvolution was tested, but it was not used for the final processing sequence. An empirical phase adjustment, based on the geologic model, was applied to some lines.

The data were processed by Argonne to 600 ms. However, none of the Argonne-processed sections appeared to show any reflection energy below approximately 300 ms. Reflections below this time were severely contaminated with surface noise at offsets less than about 400 ft, and the signal-to-noise ratio was insufficient at offsets greater than 400 ft.

We determined that the zone of greatest interest in the reflection data extended from approximately 180 ms to 280 ms. This zone encompassed a series of strong reflection events that were interpreted as being due to the top of the perched aquifer. Reflections within this time window suffered from degradation due to surface noise and refracted

energy from overlying layers. Offsets less than 300 ft contributed very little to the overall quality of the stack because of ground roll and air-coupled noise. Offsets greater than 500 ft suffered from normal moveout stretch and interfering refracted energy. The quality of the stack in the zone of interest was generally diminished if offsets less than 300 ft or greater than 500 ft were included. Hence, for most of the lines, we restricted the stack to the 300- to 500-ft band of offsets. However, if the shallower reflections (around 100 ms) needed to be brought out, we included shorter offsets.

This restriction of offsets reduced the sensitivity of the stacked data to local variations in seismic velocity and allowed us to use a smoothed areal velocity model, tied to known geology at borehole locations, for normal moveout corrections. The resulting quality of the stacked data indicates that many of the fluctuations seen in the original velocity analyses were actually due to correlations of coherent noise. The most significant variations in velocity were in lines that crossed playas, where apparent sags in underlying strata proved to be largely due to slower near-surface velocities.

. We tested and eliminated several other processing steps. F-K filtering of the stacked section sometimes reduced the residual surface noise so that offsets less than 300 ft could be included without degrading the reflection signal. The effect was not universally significant, however, so we used F-K filtering only where shallow resolution was critical. We also tested migration of the stacked section, but it did not improve resolution and was therefore not included.

The application of surface-consistent statics did not appear to improve the quality of the stack, despite evidence that at least some of the lines do in fact suffer from near-surface effects. This failure may be because the effective common midpoint fold was so small (averaging about sixfold), due to the restricted offset distribution, that no stable solution to the normal set of coupled equations was possible. We therefore excluded surface-consistent statics from the standard processing sequence. Refraction statics, which might prove beneficial near ditches or playas, were not applied.

INTERPRETATION

The reprocessed seismic lines were characterized by strong, continuous reflections occurring at arrival times that approximately correspond to the depth to groundwater. This pattern is consistent with the seismic response that would be predicted in this unconsolidated geologic section, where acoustic impedance is controlled largely by pore fluids.

The magnitude of a reflection event is determined by the change in acoustic impedance at a boundary, where the acoustic impedance is equal to the product of seismic velocity and density. In a shallow, unconsolidated section, the largest impedance contrast should occur as water-filled pores increase seismic velocities from 1,500-3,000 ft/s, the prevailing level (close to the velocity of water, which is 5,000 ft/s). Likewise, the largest density increase occurs as the pore volume, about 20-30%, takes on the density of water rather than that of air.

. The existing geologic model suggested that the presence of a consolidated caliche layer would also provide a considerable impedance contrast resulting in a strong reflection. Analysis of both reflection and refraction seismic data, however, showed that no such layer is present in the consolidated form typically associated with high seismic velocities.

Other reflection events reported on previous seismic interpretations in the area were produced from boundaries at the top of the Ogallala aquifer, at the top of a gravel within the Ogallala, and at the surface of red beds underlying the Ogallala. However, the noise recorded in the seismic data (as discussed in the section on seismic processing) prevented recovery of signal reflected from these deeper interfaces.

The predominant reflections occurring on most seismic lines had arrival times corresponding to the depth of the perched water. This interface produced a high-amplitude event that was continuous and relatively flat over much of the area. This reflection is the black peak that appears at about 200 ms on the seismic sections in Figures 7a and b.

The perched-water reflection is seen on all the seismic lines processed to date. On some of the lines, however, the reflection becomes partially or completely attenuated in segments, indicating that the perched water either is thinner than the resolution of the seismic data or is absent.

Shallow water beneath ditches

In a number of places on the seismic lines, shallow, high-amplitude reflections are seen over short distances. Many of these events are associated with a pull-up of the underlying perched-water reflection, indicating that the shallow reflection corresponds to higher velocities than in surrounding areas. Because caliche beds were expected in this area, we suspected that the high-velocity zones represented caliche accumulations. However, detailed analyses of refraction arrivals showed that the velocities in these zones were near the velocity of water, about 5,000 ft/s.

. Mapping of these shallow events showed that their occurrence corresponded to the locations of major drainage ditches. For example, Figure 7b shows shallow, high-amplitude events at shot points 260, 450, and 540. A ditch crosses this line at each of these locations. Each shallow event causes a pull-up in the underlying perched-water reflector.

The disruption in topography at a ditch location could be expected to affect the quality of seismic data, but it would not account for the water velocities measured beneath the ditches or for the significant pull-ups of underlying reflections. Therefore, we conclude that the seismic reflections indicate the presence of vadose water in the shallow section beneath the ditches. If significant amounts of water underlie the ditches, the ditches may be the source of more recharge than the surrounding interplaya surface.

Refraction data were extracted from the seismic records in an attempt to explain the apparent near-surface velocity changes in the vicinity of the drainage ditches. The first

breaks were manually selected to offsets of about 200 ft on both sides of the shot point for several records on Figure 7b. This offset distribution was sufficient to include the first arrivals through the uppermost layer, as well as refracted energy from the first layer beneath the surface layer. Generally speaking, two straight line segments were observed within this range of offsets. We interpreted the slopes of the linear segments as corresponding to the seismic velocities through the upper two layers. We calculated depths to the top of the lower layer by using a standard geometrically derived formula. These simple calculations were based on the assumption of a flat, nondipping geology.

The high-velocity zones are expressed on the unprocessed shot gathers as small humps on the sides of the refraction arrivals from the lower layer. An example of this effect is shown in Figure 8. The five traces just to the right of the dead trace, representing offsets of 80-120 ft, have first breaks that exhibit an apparent velocity of about 4,500 ft/s, considerably faster than the apparent velocity of 3,000 ft/s exhibited by traces from offsets greater than 120 ft. (Apparent velocity is the inverse of the slope of the straight line formed by connecting the first breaks of adjacent traces.)

The area around station 450 was analyzed in greater detail by using the generalized reciprocal method. Analysis of the data revealed two average velocities. The first layer extends to a depth of approximately 20 ft and has an average velocity of 1,600 ft/s. The next velocity changes do not represent layers, but rather velocity zones between shot points 463 and 467 and at shot point 475. These zones have an average velocity in excess of 3,900 ft/s and extend to a depth of at least 39 ft. However, because the refraction data are limited, whether these zones extend beyond this depth is unknown. The velocity zones may extend through the upper layer to the surface.

Playa water

Playas have been considered to be the major recharge zones around the site. Line B-1 (Figure 7a) was shot across one of these playas. Each line shows the perched-water reflection to be continuous beneath the playa. The sag of about 60 ms in the perched-water reflection as it crosses under the playa is caused by unusually slow near-surface velocities in the playa. However, a local high is seen within this sag on Line B-1 as the reflection passes under a set of high-amplitude shallow reflections between shot points 280 and 380.

We interpreted the shallow, high-amplitude events as saturated zones beneath the playa surface, with the increased seismic velocity through this water accounting for the pull-ups on deeper reflections. The effect is the same as that seen on smaller line segments across ditches.

BOREHOLE GEOPHYSICS

All of the known borehole geophysical logs were gathered and reviewed. Because the borehole geophysical logs were in a variety of computer formats, we had the digitized logs converted to ASCII, allowing us to replot the geophysical logs quickly and efficiently with a standard worksheet program.

We replotted the data from the worksheet at a larger scale to allow interpretation of the log in sufficient detail. The scales at which the logs were previously plotted were used to accommodate written descriptions of the lithology of subsurface materials. We have found that the smaller scale does not allow for the detail interpretation required.

The objective of our review and reinterpretation of the geophysical logs was to determine the adequacy of the lithologic logs and the presence or absence of subsurface water, especially in the vadose and the perched-water zones. We also analyzed geophysical

logs for the presence of the reported caliche layer and used lithologic descriptions from these borings to develop a geologic model for interpretation of seismic data.

Analysis of the geophysical well log data suggested that the upper sediments are more variable than the lithologic logs indicated. In some instances the lithologic and geophysical interpretations are contradictory. The neutron logs suggest that zones of partial water saturation may be present in the vadose zone. Such zones would indicate movement of water in the subsurface, possibly following a complicated pathway controlled by the locations of areas of enhanced infiltration (ditches) and by the heterogeneity of the underlying vadose zone lithology.

We could not confirm the presence of a well-defined caliche layer from the geophysical logs. Such a layer was apparently postulated in earlier reports on site geology without definitive data.

CONCLUSIONS

Argonne's ESC program emphasizes the analysis of any available raw field data in order to avoid unnecessary expenditures on new data acquisition. Our examination of the field tapes of an existing reflection survey allowed us to answer basic questions about the presence of the perched aquifer without resorting to a new field program. The existing field data provided useful hydrologic information. Moreover, the reprocessed data confirmed that perched water did exist beneath playas and ditches, indicating that both could be important sources of recharge.

ACKNOWLEDGMENT

This work was supported by the U.S. Department of Energy, Assistant Secretary for Environmental Management, Office of Technology Development, under contract W-31-109-Eng-38.

Table 1 Final Data Acquisition Parameters

Geophone station spacing	10 ft
Source spacing	20 ft
Geophones per station	1
Geophone frequency	100 Hz
Spread length	950 ft
Near offset	0 ft
Far offset	710 ft
Cable geometry	Unbalanced split spread
Number of recording channels	96
Sample rate	0.50 ms
Maximum record length	1 s
Low-cut filter	50 Hz, 18 dB/octave
Alias filter	360 Hz, 52 dB/octave
Common depth point fold	24
Source	Bolt LSS-3B land air gun, 5 pops per source point

Table 2 Original Processing Sequence

Step	Description
1.	Demultiplexing
2.	Recording gain removal
3.	Geometry definition
4.	Trace editing
5.	Surface-consistent deconvolution Shots: 50- to 120-Hz output minimum phase Receivers: 50- to 200-Hz output zero phase (14 dB/octave slopes)
6.	Gain recovery
7.	High-frequency spectral balancing, 30-240 Hz
8.	Optimized non-Gaussian noise estimation on shots
9.	Common midpoint gathers
10.	Datum statics application Datum = 3,520 ft Replacement Velocity = 2,000 ft/s
11.	Brute velocity analyses
12.	Removal of datum statics
13.	Daniel generalized reciprocal method refraction statics One-layer case Apply bulk shift = 0 ms before application Datum = 3,520 ft Replacement velocity = 2,000 ft/s
14.	Surface-consistent automatic statics application Pilot length = 7 traces Maximum shift limit = 4 ms
15.	Final velocity analyses
16.	Normal moveout corrections
17.	Post-moveout mute
18.	High-frequency surface-consistent automatic statics Pilot length = 7 traces Maximum shift limit = 4 ms
19.	Common-depth-point-consistent residual statics Deep gate: Pilot length = 11 traces Maximum shift limit = 2 ms Shallow gate: Pilot length = 3 traces Maximum length = 1 ms
20.	Common depth point stack: 24-fold (varying)

Table 2 Original Processing Sequence (Cont.)

Step	Description
21.	Scaling (balance): three gates 0-250 ms 250-550 ms 550-950 ms
22.	Enhanced random noise suppression filter (common-depth-point domain) Spectral balance (30-200 Hz) on data 35% signal addback
23.	Finite-difference wave equation migration
24.	Time-variant filter 0-250 ms: 20/30-135/155 Hz 450-950 ms: 15/20-90/110 Hz

Table 3 Argonne Processing Sequence

Step	Description
1.	Data input
2.	Resampling to 2 ms 125-Hz anti-alias filter applied
3.	Common midpoint sort geometry definition
4.	Trace editing
5.	Datum statics 3,550-ft datum 2,000-ft/s replacement velocity
6.	Spiking deconvolution 100-ms operator length
7.	Bandpass filter Zero-phase Butterworth: 10/18-80/36
8.	Gain Automatic gain control: 200-ms window
9.	Velocity analysis
10.	Normal moveout correction Stretch mute: 200%
11.	Stack Offsets: 300-500 ft

FIGURE CAPTIONS

Figure 1 Display of seismic field record. An automatic gain function with a sliding window of 200 ms was applied.

Figure 2 Spectral analysis of selected traces from the field record shown in Figure 1.

Figure 3 Spectral analysis of traces shown in Figure 2 after top and bottom mutes were applied, so that only reflection energy was analyzed.

Figure 4a Field record shown in Figure 1 after spectral balancing of frequencies between 30 Hz and 90 Hz.

Figure 4b Field record shown in Figure 1 after spectral balancing of frequencies between 30 Hz and 240 Hz.

Figure 5 Portion of a seismic line after original processing. The information panel at the top contains the two-way reflection times (in ms) of the reflectors used for velocity analysis; the root-mean-squared velocities (VRMS, in ft/s), derived from the normal moveout velocities used to stack the data; the interval velocities (VINT, in ft/s) obtained from the root-mean-squared velocities; and the depths (in ft) to the reflectors, calculated from the interval velocities. The depth scale on the side indicates that a reflection time of 450 ms corresponds to a depth of about 720 ft, whereas the panel at the top of the section for depth point 305 indicates a depth of 1,025 ft for 450 ms.

Figure 6 Portions of two seismic lines in the vicinity of their mutual tie point (arrow). Note the mis-ties at the aquitard and the red bed bedrock reflector. Even the

ground elevation is off by about 5 ms. The mis-ties cannot be resolved by moving one section up or down with respect to the other.

Figure 7a Line B-1, reprocessed by Argonne with the steps outlined in Table 3.

Figure 7b Line B-3, reprocessed by Argonne with the steps outlined in Table 3.

Figure 8 Shot gather from Line B-3. An automatic gain function with a sliding window of 200 ms has been applied to the data.

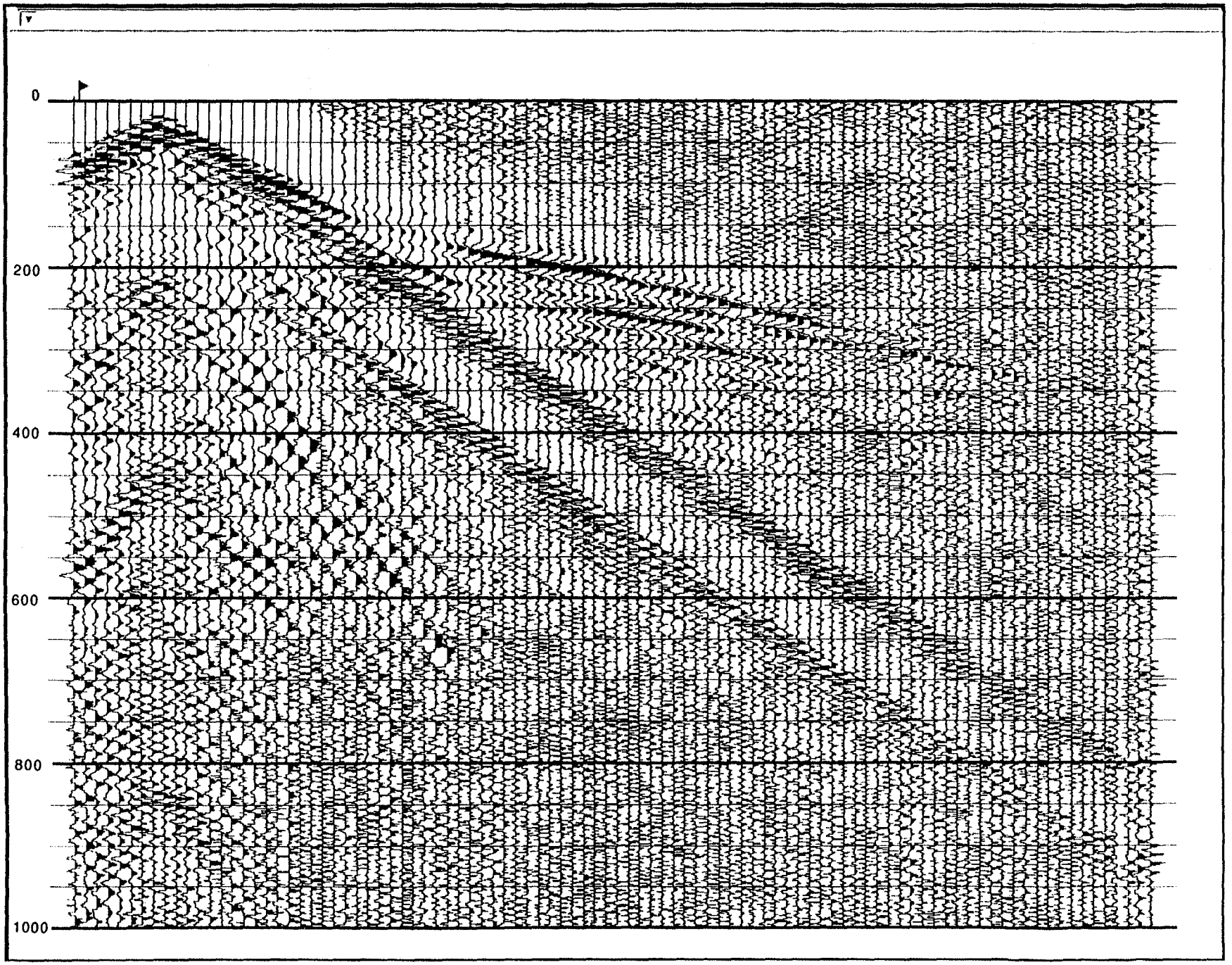

Hastings
Figure 1

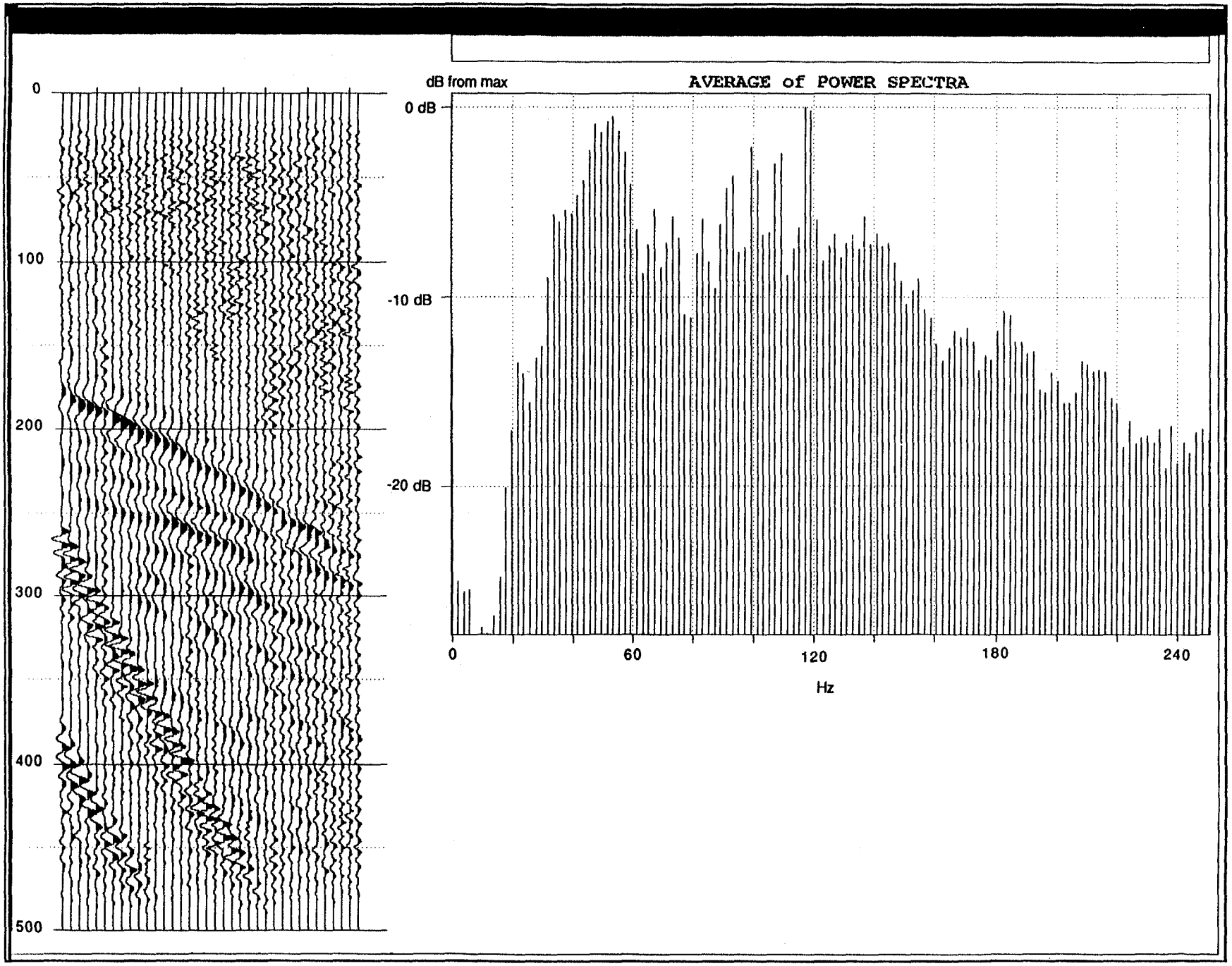

Hastings
Figure 2

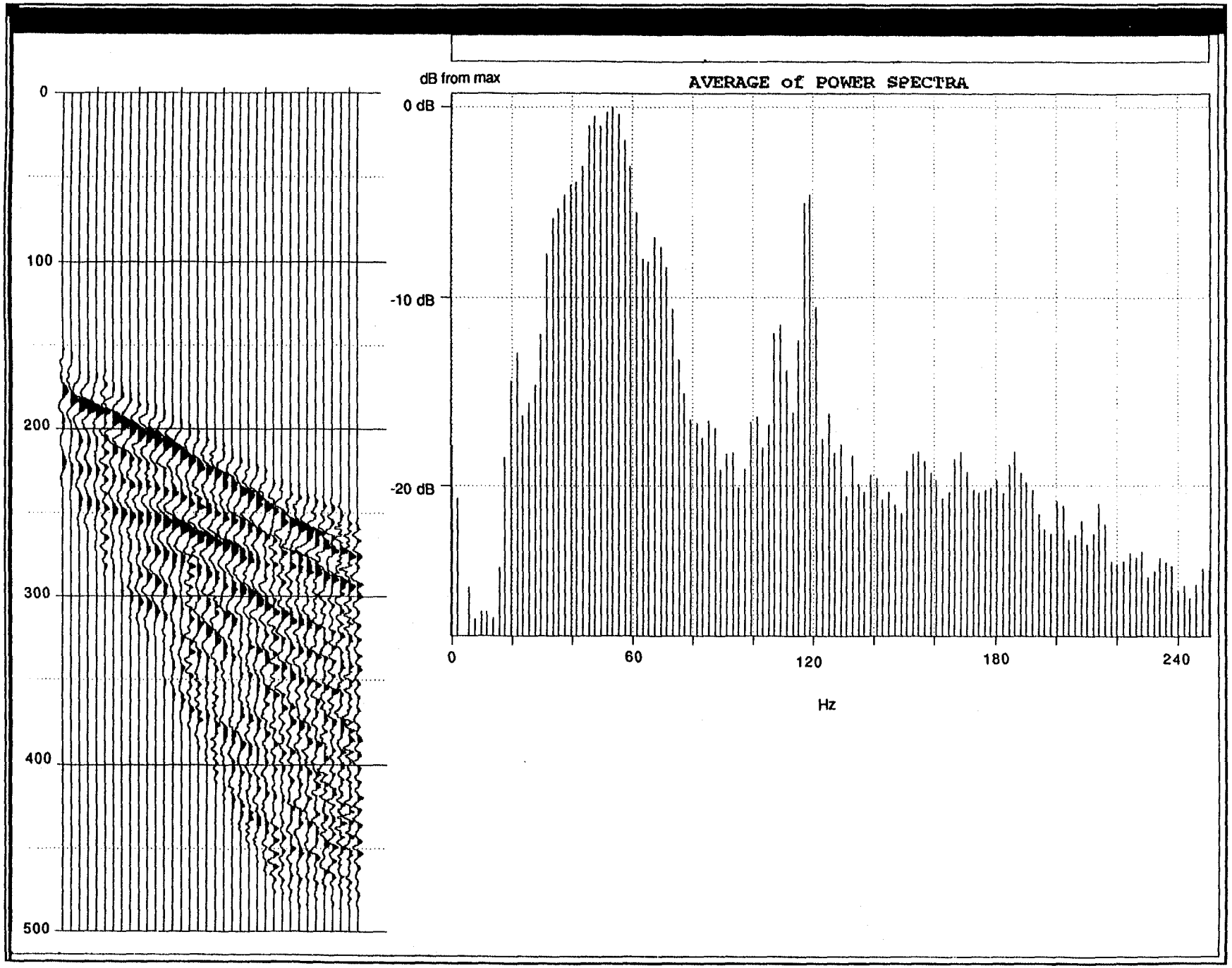

Hastings
Figure 3

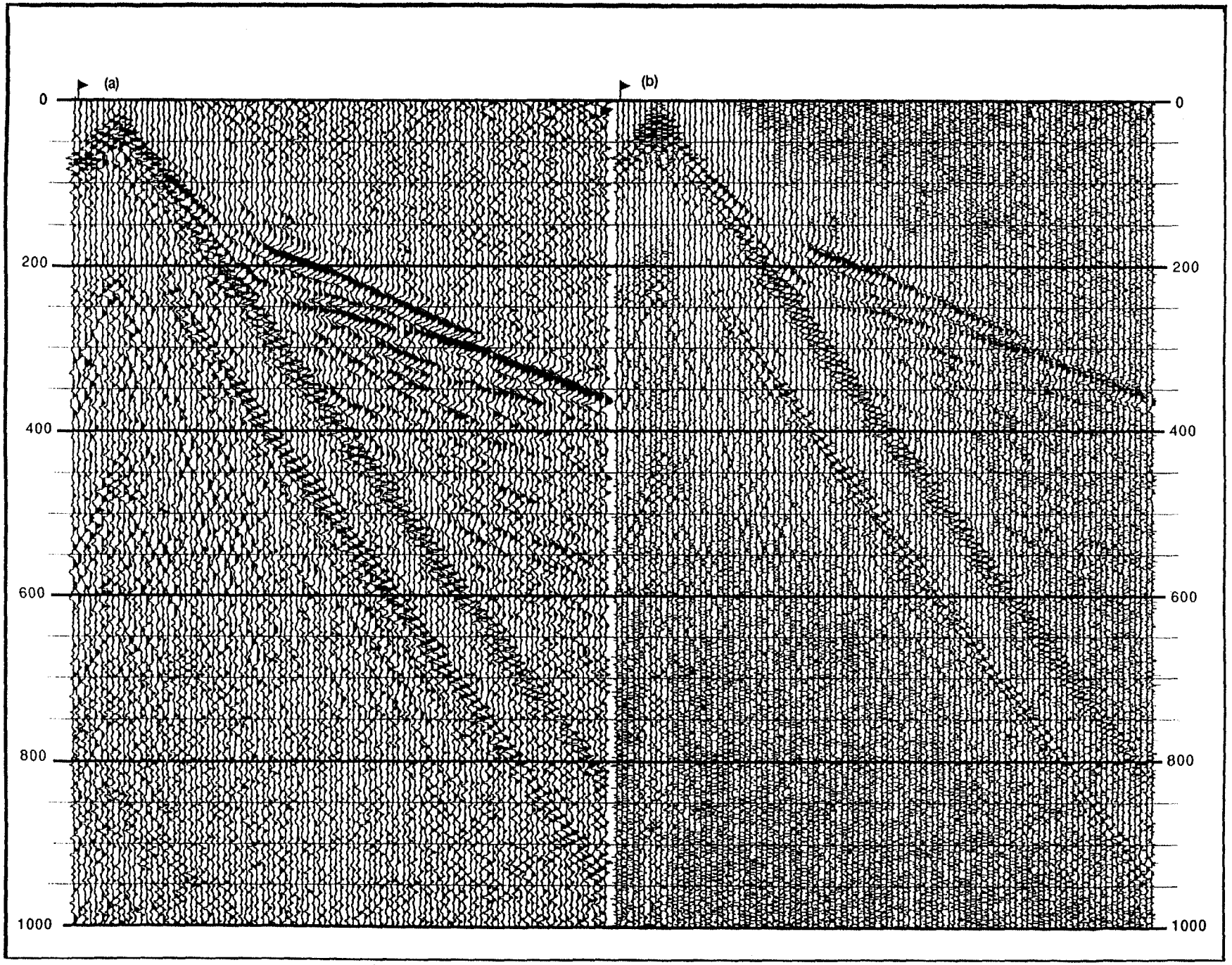

Hastings
Figure 4

TIME	VRMS	VINT	DEPTH
0	1700		0
80	2000	2000	80
115	2200	2600	126
170	2600	3282	216
210	2800	3526	286
265	3000	3665	387
295	3400	5846	475
345	4000	6496	637
385	4500	7544	788
450	5000	7289	1025
575	5500	7011	1463
715	6000	7721	2004
955	6300	7119	2858

N

305

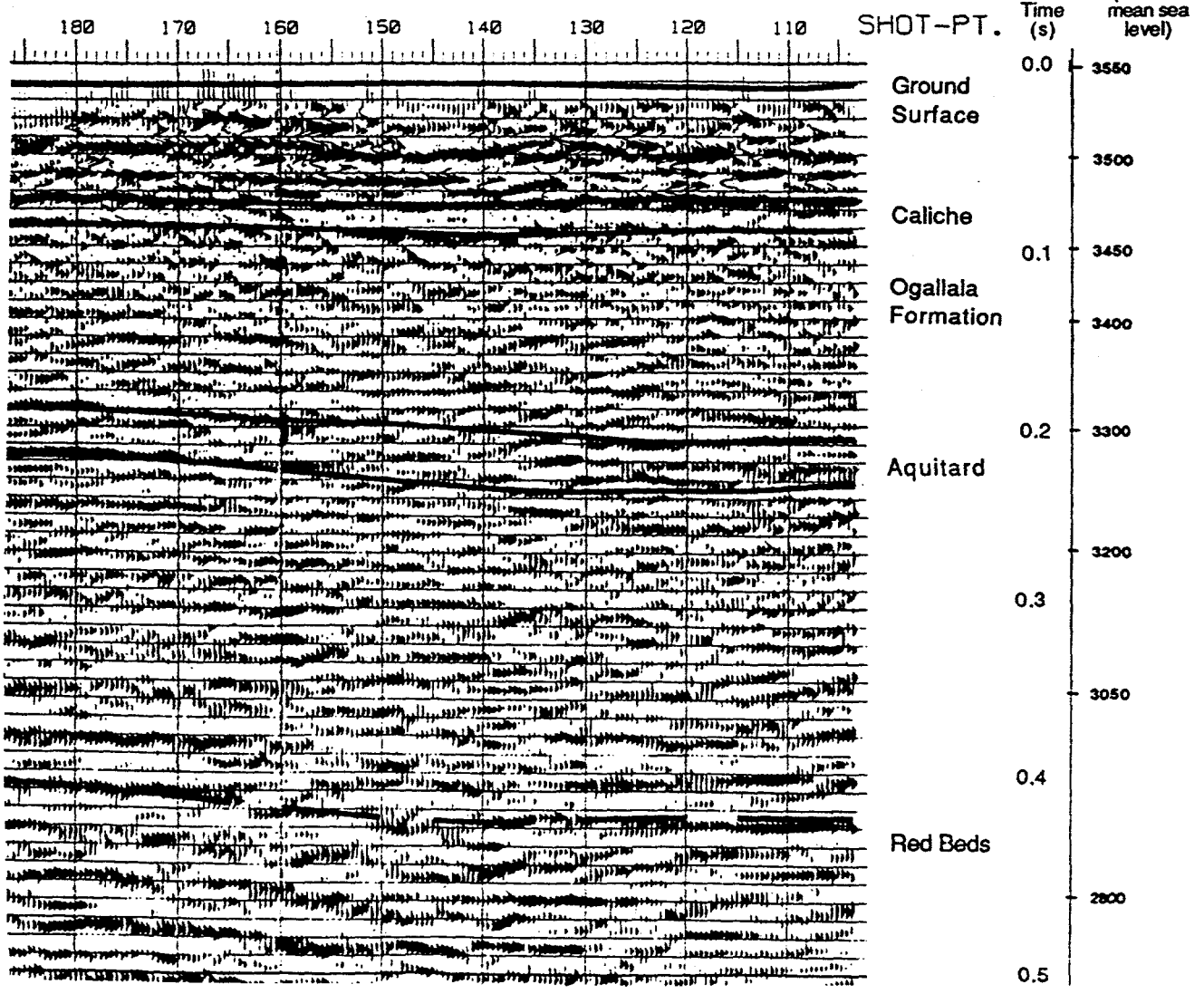

Hastings
Figure 5

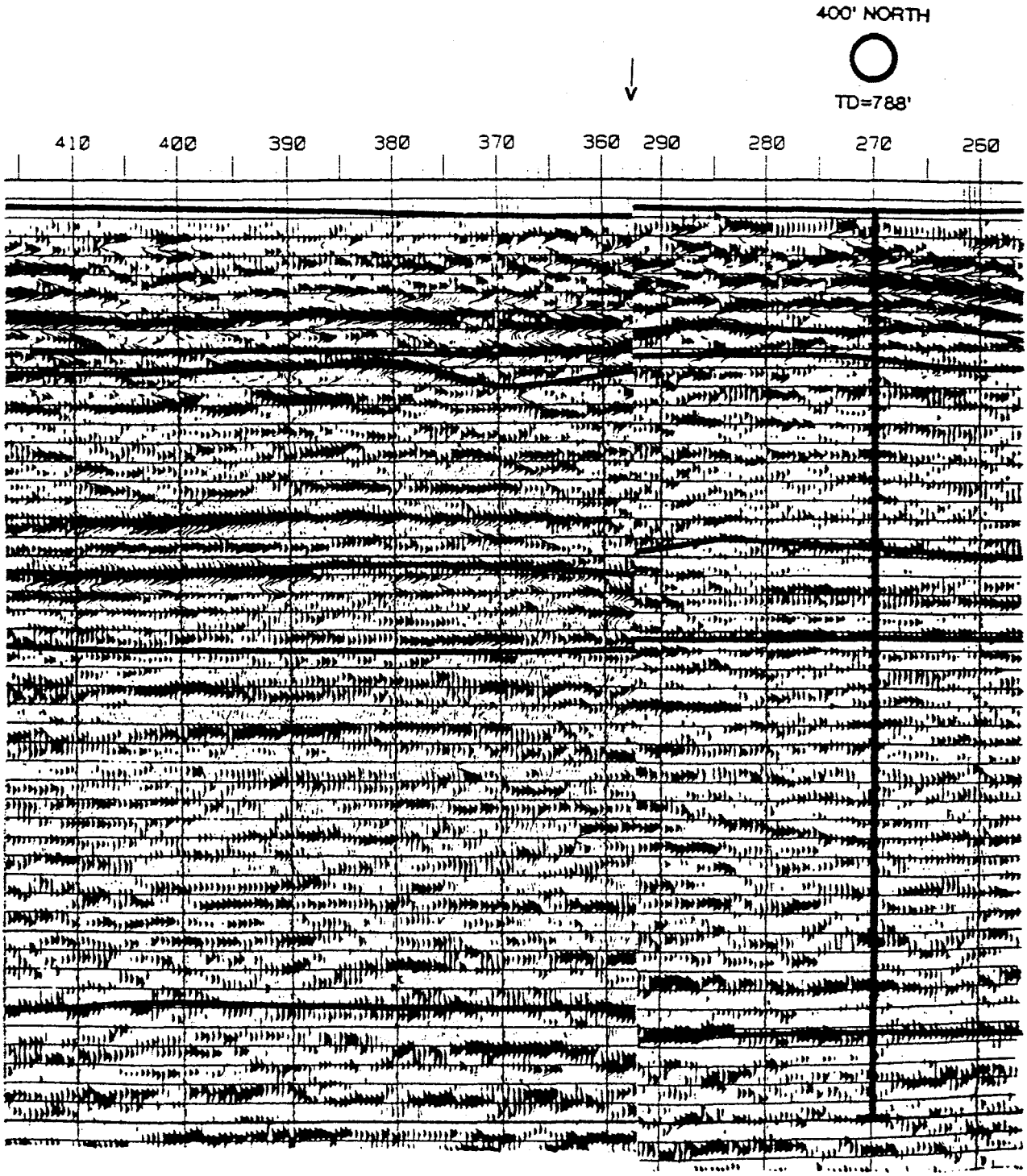

Hastings
Figure 6

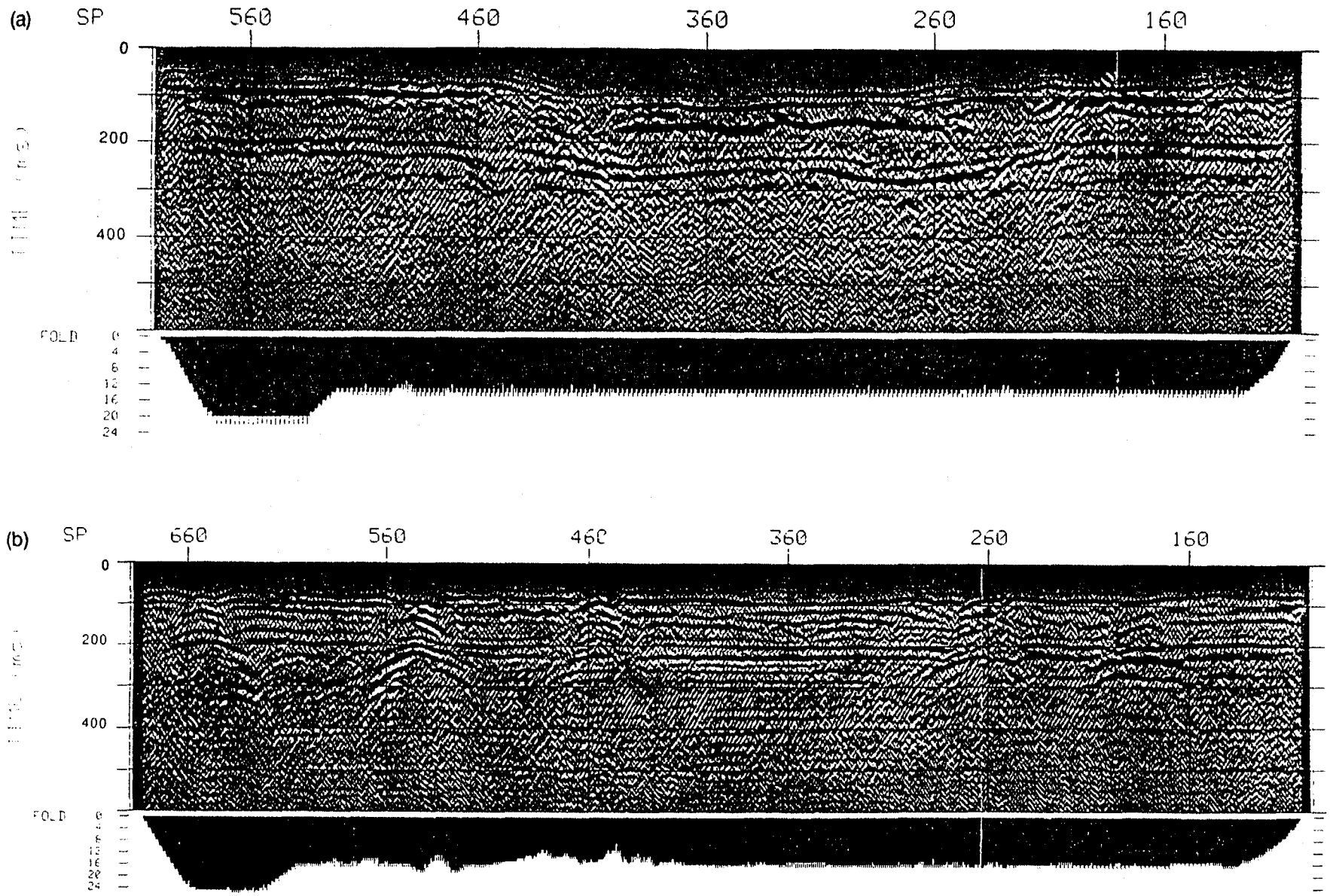

Hastings
Figure 7

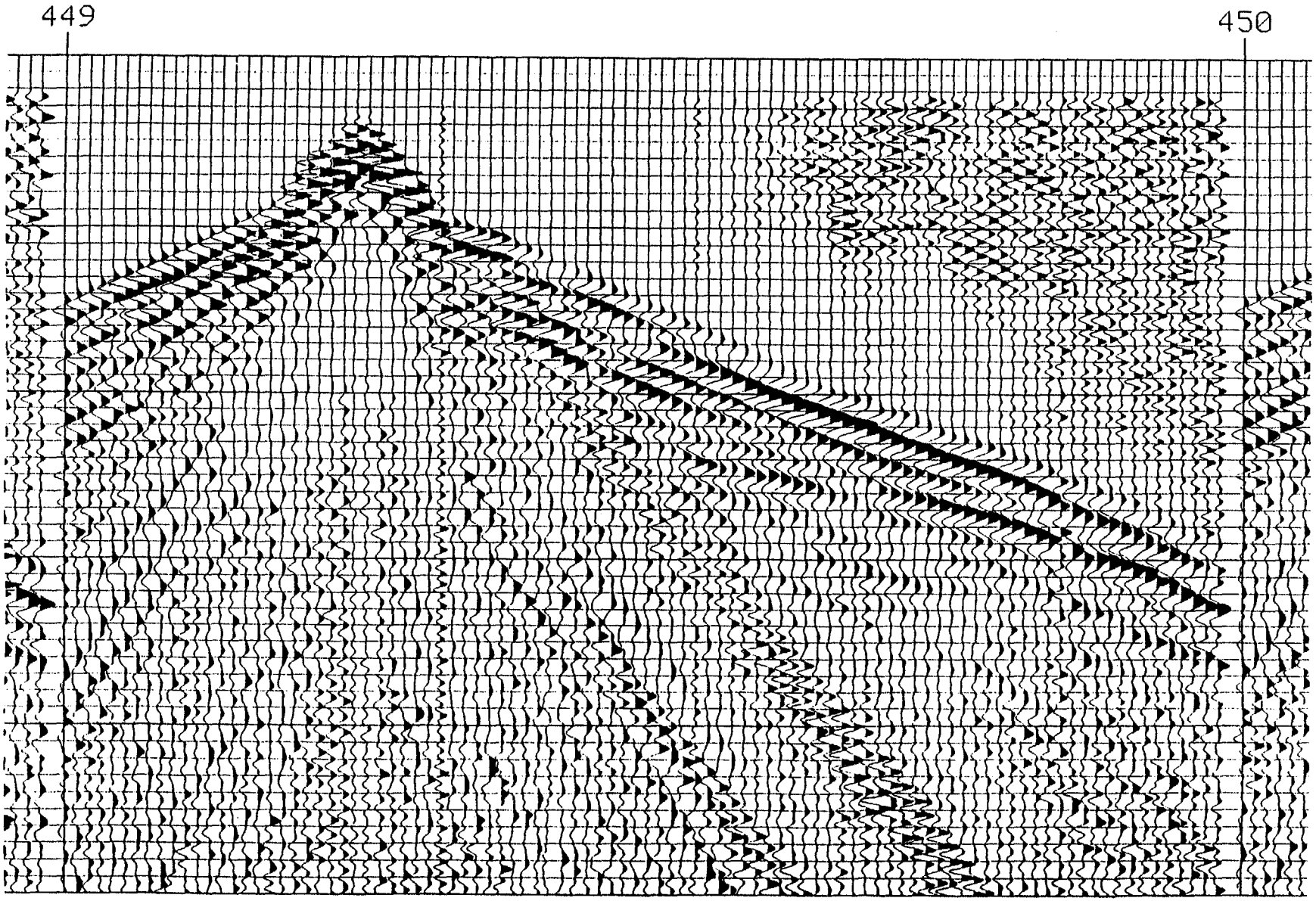

Hastings
Figure 8